HIGH-CHARGE AND HIGH-BRIGHTNESS BEAM GENERATION AT THE ADVANCED PHOTON SOURCE PHOTOINJECTOR*

Y. Sun†, T. Berenc, W. Berg, J. Calvey, J. Dooling, T. Fors, R. Hong, O. Mohsen, P. Piot, O. Ramachandran, K. P. Wootton, Y. Yang, Argonne National Laboratory, Lemont, IL, USA
T. Suzuki, Michigan State University, East Lansing, MI, USA

Abstract

The recent installation of a new photocathode drive laser has significantly improved the reliability of photoinjector operations at the Advanced Photon Source (APS), Argonne National Laboratory. The photoinjector can operate in either high-charge or high-brightness mode. The high-charge mode is ultimately intended to support direct injection from the linac into the booster ring, eliminating the need for charge accumulation performed in the Particle Accumulator Ring (PAR). In contrast, the high-brightness mode optimizes the photoemission source to produce bright, compressed electron bunches that can be delivered to the Linac Extension Area (LEA) for accelerator R&D. This paper discusses the design considerations and initial commissioning results of the photoinjector with the new laser system.

INTRODUCTION

In its current configuration, the electron beams injected into the Advanced Photon Source (APS) storage ring are generated by a thermionic RF gun, owing to its reliability. Trains of ~15–30 bunches separated by 350 ps are accelerated to 425 MeV in the S-band linear accelerator and injected into the PAR, where the bunches are merged and accumulated up to ~20 nC single bunch for the injection to booster; see Fig. 1. In the booster, the bunch is accelerated to 6 GeV prior to injection into the APS storage ring [1, 2].

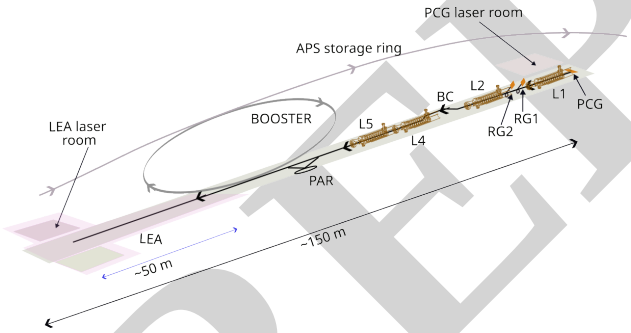

Figure 1: Overview of the APS injection complex chain. The labels "PCG", "RG", "L", and "BC" refer to the photocathode rf gun, thermionic rf gun, linac sections, and bunch compressor chicane, respectively.

In addition to the nominal and spare thermionic radiofrequency (rf) guns (RG1 and RG2), the APS linac also houses a rf photoemission source (PCG) of similar design to the LCLS rf gun [3, 4]. The photoinjector's operation has been limited over the years by the performance of the photocathode laser system. In 2025, a new commercial laser system was commissioned, enabling the generation of electron bunches with charges $Q \in [0.1, 2]$ nC for R&D purposes and possibly for direct injection into the PAR. In the longer term, further upgrades to the laser and/or photocathode could support the generation of ~20 nC bunches – potentially arranged as a multi-bunch train from the linac – enabling direct injection from the linac into the booster and storage rings while bypassing the PAR, which represents a current bottleneck in the APS injection chain due to bunch length blowup at higher single bunch charge [2]. Additionally, the photoinjector can be optimized to produce high-brightness electron bunches with sub-micrometer normalized emittances at $Q = 100$ pC.

NEW PHOTOCATHODE-LASER SYSTEM

The laser system was upgraded to an Ytterbium-doped Potassium Gadolinium Tungstate (Yb:KGW) PHAROS laser from LIGHTCONVERSION capable of producing amplified infrared (IR) pulses with energies up to 4 mJ at $\lambda = 1030$ nm. The laser is comprised of an integrated oscillator operating at 68 MHz (42nd subharmonic of 2856 MHz reference signal) and a regenerative amplifier. The oscillator cavity is phase-locked to the reference signal using a commercial synchronization system (PHASELOCK module from TEM Messtechnik). Initial in-loop synchronization measurements indicate ~ 300 fs (rms) timing jitter; see Fig. 2. The regenerative amplifier is operated at 1.2 kHz and a pulse picker extracts laser pulses at 30 Hz timed to coincide with the linac RF macropulses. In its short-pulse settings the system produces ~450-fs (FWHM) amplified IR pulses. Following frequency quadrupling via two cascaded second-harmonic

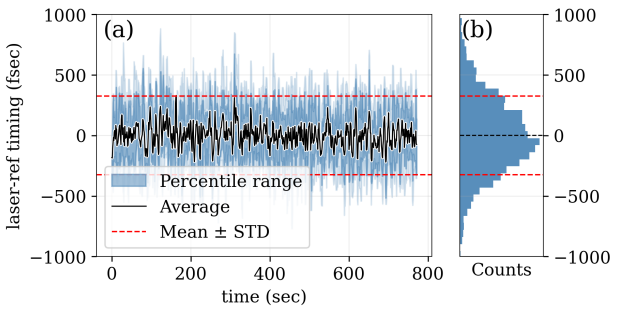

Figure 2: Example of timing jitter between the laser oscillator and the 2856-MHz reference signal, measured using an in-loop comparative phase detector.

* This material is based upon work supported by Laboratory Directed Research and Development (LDRD) funding from Argonne National Laboratory, provided by the Director, Office of Science, of the U.S. Department of Energy under Contract No. DE-AC02-06CH11357.
† yinesun@anl.gov

generation stages, the IR laser pulse is converted into an ultraviolet (UV) pulse 257.5 nm with duration ~ 220 fs (FWHM). Finally, the UV pulses are sent to the photocathode through a 6 m optical transport line with relay-imaging optics.

EXPECTED PERFORMANCES

Brightness is usually described in term of 6D brightness [5] $B_{6d} \equiv Q/\Gamma$ where Q is the bunch charge and Γ the 6D phase-space volume which, for a bunch with no cross-plane coupling, can be written as the product of the horizontal- vertical- and longitudinal-plane emittance, i.e., $\Gamma = \varepsilon_x\varepsilon_y\varepsilon_z$ (throughout this note the emittances are defined as the *normalized emittances*). Here we consider the 5D brightness defined as $B_{5d} \equiv I/\varepsilon_x\varepsilon_y$, where $I \equiv Q/\tau$ refers to the bunch peak current (here τ is the bunch duration). The brightness scales favorably with the electric field applied on the photocathode surface typically as [6] $B_{5d} \propto E_0^{\nu}$ where ν is a parameter depending on the transverse-to-longitudinal aspect ratio of the bunch at emission.

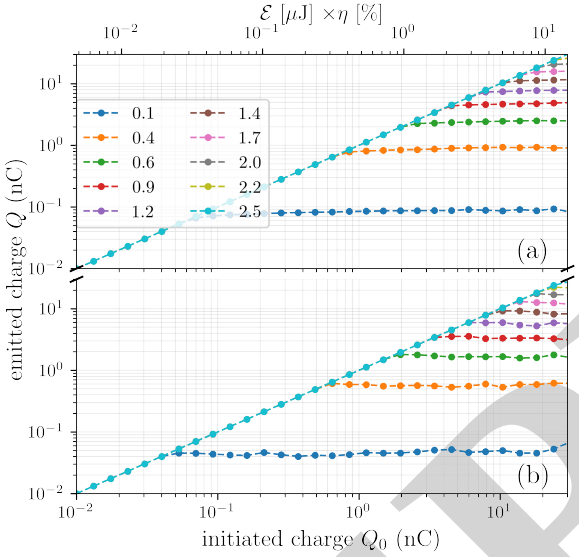

Figure 3: Emitted charge 0.5-m downstream of the RF gun for different laser-spot sizes on the photocathode for the a Gaussian (a) and plateau (b) temporal distribution with same rms pulse duration $\sigma_t = 3.2$ ps. The horizontal axis represent the initiated charge Q_0. The label associated with the traces are the rms laser size in units of mm.

The beam-dynamics simulations presented below were conducted using ASTRA [7] for energies up to ~150 MeV where the distribution can be passed to other simulation program such as ELEGANT [8]. This "hand-shake" energy corresponding to downstream of linac L2 was selected to ensure the beam is thermalized and space-charge effects do not significantly impact the beam dynamics anymore. The objectives were to minimize the transverse-emittance ε and a bunch length σ_z. In addition, a constraint implemented as an objective was to minimize macroparticle loss (a circular aperture with a diameter of 30 mm was implemented throughout the simulation domain). The bunch length objective is important for applications that require enhanced 5-D brightness. High-charge operation for injection in the APS complex will likely require low energy spread. This optimization were performed over various bunch charges up to $Q = 15.34$ nC required for timing-mode operation of the APS (i.e. 200-mA stored beam with a 48-bunch pattern).

The charge-extraction plots for both laser temporal distributions (Gaussian and flat-top, each with 3 ps rms duration) as a function of transverse laser spot size and initiated charge Q_0 are shown in Fig. 3. For a given UV-laser pulse energy E and quantum efficiency η, the initiated charge is $Q_0 = \eta[\%]\frac{\lambda[\text{nm}]E[\mu\text{J}]}{124}$.

The gun operates at $E_0 = 120$ MV/m and $\varphi_0 = 40°$ relative to the zero-crossing phase ($f = 2856$ MHz). Calculations confirm that $Q \geq 10$ nC can be extracted for laser-spot rms sizes $\sigma \geq 1.4$ mm, provided a high-QE photocathode is used, such as magnesium [9], a semiconductor [10], or a patterned metallic cathode exploiting plasmonic resonance. Both temporal distributions reach the charge-saturation limit at approximately the same initiated charge for a given spot size, consistent with equal incident laser energy.

Figure 4 summarizes the Pareto fronts associated with the minimization of transverse emittance and bunch length downstream of L2 for the three charge cases considered in this study. The results for the Gaussian and flat-top laser distributions are presented respectively in Fig. 4(a) and 4(b). For $Q = 0.1$ nC, transverse emittances at the sub-micrometer level are attained, with the plateau distribution notably supporting emittance values approaching 150 nm. Figure 4 indicate that the 5-D brightness associated with various Pareto fronts (shown as color levels) can attain ~10^{15} A.m^{-2} at 100 pC – a value comparable to values achieved in state-of-the-art electron linacs driving free-electron laser facilities. Higher charge generally yields lower brightness because the rate at which bunch length and transverse emittances grow with charge outpaces the charge gain itself.

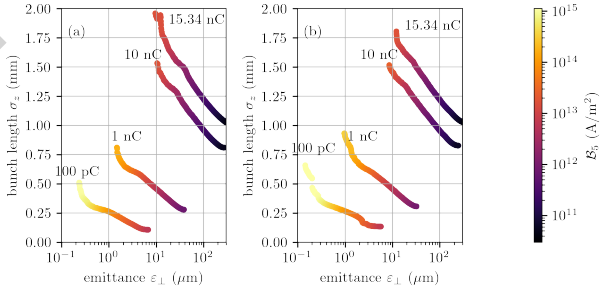

Figure 4: The tradeoff between the transverse emittance and bunch length downstream of linac L2 for the case of an initial Gaussian (a) and plateau (b) temporal laser distributions. The color coding indicates the attained 5-D brightness.

FIRST-BEAM GENERATION

During APS Run 2026-1, commissioning of the integrated photoinjector system was initiated. The photocathode drive laser was aligned and delivered to the photoinjector, and

preliminary data was acquired to characterize the system stability. Beam-based measurements confirmed that the laser and RF systems operated within acceptable parameters. The transverse phase space of the extracted electron bunches is not optimized during the commissioning stage as the control and diagnostics of the laser spot size on the photocathode is yet to be implemented. Nevertheless, the system demonstrated the generation of bunch charges in excess of 1.5 nC with UV pulse energy $E \simeq 300\,\mu J$ in the laser room; see typical gun rf phase scan in Fig. 5.

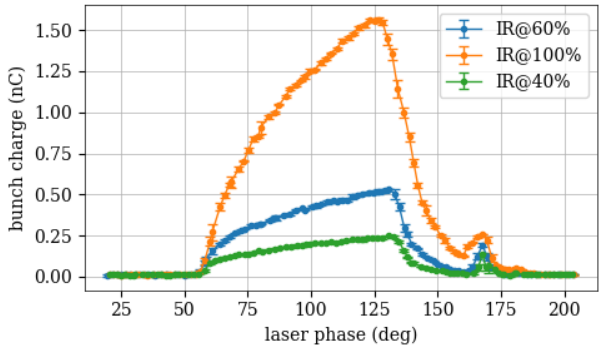

Figure 5: Phase scan measured for different IR-pulse energies (100% corresponds to 4 mJ).

Finally, the beam was sent to a dispersive section downstream of the RF gun and the system was operated for 24 hours and the recorded stability appears in Fig. 6 where the charge was limited below 1 nC by attenuating the laser. The repetition rate was set to 30 Hz. During this initial test, the laser showed acceptable performance, in addition to the low time jitter (see Fig. 2), the electron-bunch energy was measured and stability of 3.2% and charge remains at $718 \pm 16\,pC$; see Fig. 6(a) and (b) respectively.

The overall performance is promising and suggests that the system could support reliable operation, including for storage ring injection within the current injection chain. Such a configuration would enable a simpler interleaving scheme using the PCG beam only for the simultaneous operations of the SR and LEA, significantly reducing the complexity of the original plan [11], which relied on interleaving RG2 and PCG beams.

OUTLOOKS

With the new photocathode laser system integrated, the next running period APS Run 2026-2 will focus on producing high-quality electron bunches and accelerating them through the linac for UV spot size on the photocathode and a pulse shaper using alpha-BBO crystals to produce a plateau temporal distribution for improved emittance [12, 13]. In addition, preliminary simulations regarding the injection of a train of four 5-nC bunches for direct injection into the booster ring are promising, and the concept will be tested, albeit at lower charge (limited by the current laser system), to confirm the possibility of merging this bunch train into a single bunch during energy ramping [2]. Beyond investigating the merging process of the injected bunches, the main

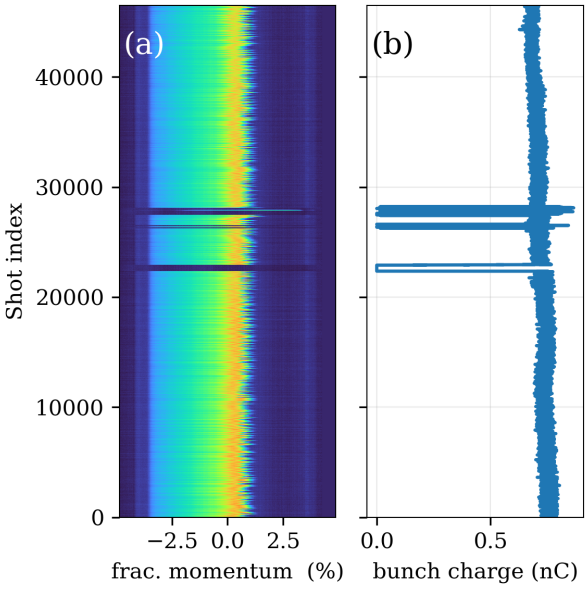

Figure 6: Waterfall plot of the energy distribution in the dispersive-section YAG screen (a) and corresponding current (b) measured over 11 hours. The missing shots around 25000 and 27000 correspond to RF trips or loss of lock.

purpose of such a test will be to validate the timing scheme needed for direct injection from the linac into the booster ring, as the frequencies of these two systems do not have a harmonic relationship and the direct injection timing system is therefore critical for the success of direct injection. The injection-extraction timing system [14] (IETS) will require some modifications.

In parallel to these studies, the photoinjector is expected to support a series of experiments in the Linac Extension Area (LEA) [15] starting during APS Run 2026-3. The experiments include tests of mm-wave accelerating structures, R&D on novel fast gamma-ray detectors, THz generation, and in the longer term beam-laser interactions (e.g., seeded FEL concepts).

ACKNOWLEDGMENTS

The computing resources utilized for this research were provided by IMPROV, a high-performance computing cluster operated by the Laboratory Computing Resource Center (LCRC) at Argonne National Laboratory (ANL). We would like to thank APS technical groups for their support.

REFERENCES

[1] J. Calvey *et al.*, "Operation of the APS-U injectors with high single bunch charge", in *Proc. NAPAC'25*, Sacramento, CA, USA, Aug. 2025, pp. 20–26. doi:10.18429/JACoW-NAPAC2025-MOYN01

[2] J. Calvey *et al.*, "High Charge Operation and Future Upgrades of the APS-U Injector Chain", presented at IPAC'26, Deauville, France, May 2026, paper TUO2M04, this conference.

[3] R. Alley *et al.*, "The design for the LCLS RF photoinjector", *Nucl. Instrum. Methods Phys. Res. Sect. A*, vol. 429, no. 1, pp. 324–331, Jun. 1999. doi:10.1016/S0168-9002(99)00072-8

[4] Y. Sun *et al.*, "Commissioning of the Photo-Cathode RF Gun at APS", in *Proc. FEL'14*, Basel, Switzerland, Aug. 2014, paper THP039, pp. 803–806. https://proceedings.jacow.org/FEL2014/papers/thp039.pdf

[5] S. Di Mitri, "On the importance of electron beam brightness in high gain free electron lasers", *Photonics*, vol. 2, no. 2, pp. 317–341, 2015. doi:10.3390/photonics2020317

[6] D. Filippetto, P. Musumeci, M. Zolotorev, and G. Stupakov, "Maximum current density and beam brightness achievable by laser-driven electron sources", *Phys. Rev. Spec. Top. Accel Beams*, vol. 17, no. 2, p. 024201, Feb. 2014. doi:10.1103/PhysRevSTAB.17.024201

[7] K. Flöttmann, ASTRA – A Space Charge Tracking Algorithm, Mar. 2017, http://www.desy.de/~mpyflo/.

[8] M. Borland, "ELEGANT: A Flexible SDDS-Compliant Code for Accelerator Simulation", in *Proc. ICAP 2000*, 2000. doi:10.2172/761286

[9] T. Nakajyo, J. Yang, F. Sakai, and Y. Aoki, "Quantum Efficiencies of Mg Photocathode under Illumination with 3rd and 4th Harmonics Nd: $LiYF_4$ Laser Light in RF Gun", *Jpn. J. Appl. Phys.*, vol. 42, no. 3R, p. 1470, Mar. 2003. doi:10.1143/JJAP.42.1470

[10] S. H. Kong, J. Kinross-Wright, D. C. Nguyen, and R. L. Sheffield, "Photocathodes for free electron lasers", *Nucl. Instrum. Methods Phys. Res. Sect. A*, vol. 358, no. 1, pp. 272–275, Apr. 1995. doi:10.1016/0168-9002(94)01425-6

[11] S. Shin, Y. Sun, J. Dooling, M. Borland, and A. Zholents, "Interleaving lattice for the Argonne Advanced Photon Source linac", *Phys. Rev. Accel. Beams*, vol. 21, no. 6, p. 060101, Jun. 2018. doi:10.1103/PhysRevAccelBeams.21.060101

[12] S. Zhou *et al.*, "Efficient temporal shaping of ultrashort pulses with birefringent crystals", *Appl. Opt.*, vol. 46, no. 35, pp. 8488–8492, Dec. 2007. doi:10.1364/AO.46.008488

[13] J. G. Power and C. Jing, "Temporal Laser Pulse Shaping for RF Photocathode Guns: The Cheap and Easy way using UV Birefringent Crystals", *AIP Conf. Proc.*, vol. 1086, no. 1, pp. 689–694, Jan. 2009. doi:10.1063/1.3080991

[14] J. Calvey *et al.*, "APS Upgrade booster commissioning", in *Proc. IPAC'24*, Nashville, TN, USA, May 2024, pp. 1232–1235. doi:10.18429/JACoW-IPAC2024-TUPG07

[15] K. P. Wootton *et al.*, "The Linac Extension Area at the Advanced Photon Source", *J. Instrum.*, vol. 19, no. 07, T07002, Jul. 2024. doi:10.1088/1748-0221/19/07/T07002